Aircraft trajectory tracking by nonlinear spatial inversion

Hakim Bouadi, Felix Mora-Camino

Aircraft Trajectory Tracking by Nonlinear Spatial Inversion

Hakim Bouadi* and F. Mora-Camino†

MAIAA, Automation Research Group, National Civil Aviation Institute, Toulouse, 31000, France

With the growth of civil aviation traffic, enhanced accuracy performances are required from guidance systems to maintain efficiency and safety in flight operations. This communication proposes a new representation of aircraft flight dynamics at approach for landing and a space-based nonlinear dynamic inversion control technique for the guidance of transportation aircraft. The main novelty is that the adopted independent variable is distance to land which allows the development of a new guidance approach with a perspective for improved performance.

Nomenclature

x	Longitudinal displacement, m
z	Altitude, m
V_{air}	Airspeed, m/s
V_G	Ground speed, m/s
γ_{air}	Flight path angle w.r.t airspeed, rad
θ	Pitch angle, rad
α	Angle of attack, rad
L	Lift force, N
D	Drag force, N
T	Thrust force, N
C_Z	Lift force coefficient
C_X	Drag force coefficient
m	Mass, Kg
q	Pitch rate, rad/s
M	Pitch moment, N.m
I_y	Pitch inertia moment, Kg.m^2
ρ	Air density, Kg/m^3
S	Wing surface area, m^2
g	Gravity acceleration, m/s^2
τ	Engine time constant , s
T_C	Throttle setting , rad
δ_e	Elevator deflection , rad
w_x	Longitudinal wind component , m/s
w_z	Vertical wind component , m/s
Subscript	
k	Variable number

I. Introduction

With the growth of civil aviation traffic capacity, safety and environmental considerations urge today for the development of guidance systems with improved accuracy for spatial trajectory tracking. This should induce increased capacity by allowing safe operations in accordance with a minimum separation standards while trajectory dispersion resulting in extended noise impacts on surrounding communities should be reduced.

Current civil aviation guidance systems operate with real time corrective actions to maintain the aircraft trajectory as close as possible to the planned trajectory (Miele, A. et al.,1986a), (Miele, A. et al.,1986b). Wind is one of the main causes of guidance errors (Psiaki, M.L. and Stengel, R.F.1985), (Miele, A. et al.,1990), (Psiaki, M.L. and Stengel, R.F.1991). These guidance errors are detected by navigation systems whose accuracy have known large improvements with the hybridization of inertial units with satellite information. However, until today a high precision guidance remains difficult to be achieved (Stengel, R.F.1993), (Singh, S.N. and Rugh, W.J.1972). Covariance of tracking errors (Sandeep S, Mulgund and Robert F, Stengel.1996) still large and one reason is that time-based control laws are used to track space referenced trajectories (Psiaki, M.L.1987), (Psiaki, M.L. and Park, K.1992).

In this communication, we adopt a representation of aircraft flight dynamics where a different independent variable, distance to land, is considered to be made available online by the navigation system with acceptable accuracy. Here we treat more particularly the problem of trajectory tracking in the vertical plane for an aircraft at approach for landing.

*Phd Student, Air Transportation Department, ENAC, 07, Avenue Edouard Belin, 31400 Toulouse, France

†Professor, Air Transportation Department, ENAC, 07, Avenue Edouard Belin, 31400 Toulouse, France

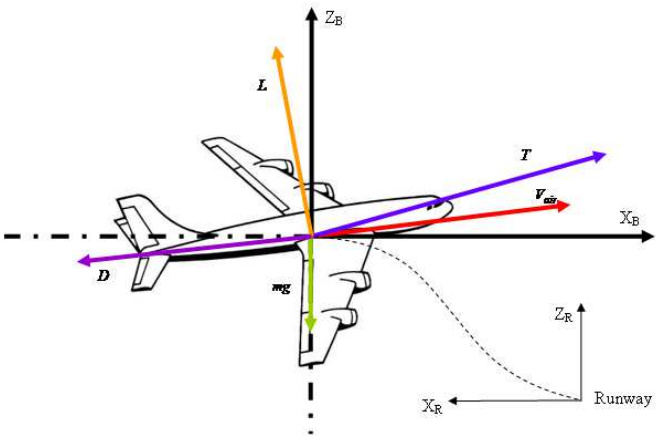

Figure 1. Aircraft forces

A nonlinear inverse control law based on the proposed space representation of flight dynamics is established. Control objectives for trajectory tracking in the space and the time frame are discussed and compared.

A wind model has been adopted and simulations have been performed in the case of a manoeuver similar to a continuous descent approach (CDA). Under different wind conditions, space and time nonlinear inverse (NLI) control laws have been used to track altitude and airspeed reference trajectories. Simulation results allow then to compare the performances of the two different guidance approaches.

II. Space Referenced Vertical Guidance Dynamics

The motion of an approach/descent transportation aircraft along a landing trajectory will be referenced with respect to a RRF (Runway Reference Frame) where its origin is located at the runway entrance (Fig. 1).

The vertical plane components of the inertial speed are such as:

$$\dot{x} = -V_{air}\cos\gamma_{air} + w_x \tag{1a}$$

$$\dot{z} = V_{air}\sin\gamma_{air} + w_z \tag{1b}$$

and inversely:

$$V_{air} = \sqrt{(\dot{x} - w_x)^2 + (\dot{z} - w_z)^2} \tag{2a}$$

$$\gamma_{air} = -\arctan\left(\frac{\dot{z} - w_z}{\dot{x} - w_x}\right) \tag{2b}$$

where x and z are the vertical plane coordinates of the aircraft center of gravity in the runway reference system, V_{air} is the airspeed modulus, γ_{air} is the airspeed path angle, w_x and w_z are the wind components in the RRF.

Adopting classical assumptions such as the RRF being an inertial frame, local flatness of the Earth, constant aircraft mass. The translational acceleration equations can be written as:

$$m\ddot{x} = -T\cos\theta + D(z, V_{air}, \alpha)\cos\gamma_{air} + L(z, V_{air}, \alpha)\sin\gamma_{air} \tag{3a}$$

$$m\ddot{z} = T\sin\theta - D(z, V_{air}, \alpha)\sin\gamma_{air} - mg + L(z, V_{air}, \alpha)\cos\gamma_{air} \tag{3b}$$

T, D and L are respectively the thrust, drag and lift forces. The lift and drag forces are given by:

$$L = \frac{1}{2}\rho(z)V_{air}^2 S C_Z \tag{4a}$$

$$D = \frac{1}{2}\rho(z)V_{air}^2 S C_X \tag{4b}$$

where $\rho(z)$, S, C_Z and C_X represent the air density with respect to the altitude, the wing surface area, the lift and drag

coefficients, respectively.

$$C_Z = C_{Z_0} + C_{Z_\alpha}\alpha \tag{5a}$$
$$C_X = C_0 + C_1\alpha + C_2\alpha^2 \tag{5b}$$

According to the polar model, the aerodynamic parameters C_0, C_1 and C_2 are such as:

$$C_0 = C_{X_0} + kC_{Z_0}^2 \tag{6a}$$
$$C_1 = 2kC_{Z_0}C_{Z_\alpha} \tag{6b}$$
$$C_2 = kC_{Z_\alpha}^2 \tag{6c}$$

Assuming first order dynamics with time constant τ for the engines, we get between commanded thrust T_C and effective thrust T the following relation:

$$\dot{T} = \frac{1}{\tau}(T_C - T) \tag{7}$$

Under the above assumptions, the pitch rate is given by:

$$\dot{\theta} = q \tag{8}$$

Equations $(3a)$ and $(3b)$ can be rewritten in the aircraft airspeed frame such as:

$$\dot{V}_{air} = \frac{1}{m}\left[T\cos\alpha - D(z, V_{air}, \alpha) - mg\sin\gamma_{air} + m\left(\dot{w}_x\cos\gamma_{air} - \dot{w}_z\sin\gamma_{air}\right)\right] \tag{9a}$$
$$\dot{\gamma}_{air} = \frac{1}{mV_{air}}\left[T\sin\alpha + L(z, V_{air}, \alpha) - mg\cos\gamma_{air} - m\left(\dot{w}_x\sin\gamma_{air} + \dot{w}_z\cos\gamma_{air}\right)\right] \tag{9b}$$

where α denotes the angle of attack with:

$$\alpha = \theta - \gamma_{air} \tag{10}$$

Considering that during an approach/descent without holding manoeuvers of an aircraft $x(t)$ is invertible and that the ground speed at position x is given by:

$$V_G = \dot{x} = -V_{air}\cos\gamma_{air} + w_x \tag{11}$$

it is possible to express during these manoeuvers all the flight variables with respect to x and its derivatives.

Here the following notation is adopted: $\frac{d^k *}{dx^k} = *^{[k]}$ and the guidance dynamics can be written as:

$$z^{[1]} = \frac{dz}{dx} = \frac{dz}{dt}\frac{dt}{dx} = \frac{V_{air}\sin\gamma_{air} + w_z}{V_G} \tag{12a}$$
$$\theta^{[1]} = \frac{q}{V_G} \tag{12b}$$
$$T^{[1]} = \frac{T_C - T}{\tau V_G} \tag{12c}$$
$$V_{air}^{[1]} = \frac{1}{mV_G}\left[T\cos\alpha - D(z, V_{air}, \alpha) - mg\sin\gamma_{air} + m\left(\dot{w}_x\cos\gamma_{air} - \dot{w}_z\sin\gamma_{air}\right)\right] \tag{12d}$$
$$\gamma_{air}^{[1]} = \frac{1}{mV_{air}V_G}\left[T\sin\alpha + L(z, V_{air}, \alpha) - mg\cos\gamma_{air} - m\left(\dot{w}_x\sin\gamma_{air} + \dot{w}_z\cos\gamma_{air}\right)\right] \tag{12e}$$

then, with respect to $z^{[2]}$ we get:

$$z^{[2]} = \frac{1}{{V_G}^2}\left[\left(V_{air}^{[1]}\sin\gamma_{air} + V_{air}\gamma_{air}^{[1]}\cos\gamma_{air} + w_z^{[1]}\right)V_G - \left(V_{air}\sin\gamma_{air} + w_z\right)V_G^{[1]}\right] \tag{13}$$

The independent inputs to the above flight dynamics are q, T_C, w_x and w_z, where wind components w_x and w_z operate as external disturbances while q is the result of pitch control and T_C is the engine thrust setting.

Note that, the space-based state equation related to the pitch is such as:

$$q^{[1]} = \frac{dq}{dt}\frac{dt}{dx} = \frac{\dot{q}}{V_G} = \frac{M}{I_y V_G} \tag{14}$$

where M, I_y denote respectively the pitch moment and inertia moment according to the aircraft lateral axis:

$$M = \frac{1}{2}\rho(z)V_{air}^2 S\overline{c}\left(C_{m_0} + C_{m_\alpha}\alpha + C_{m_q}\frac{q\overline{c}}{2V_{air}} + C_{m_{\delta_e}}\delta_e\right) \tag{15}$$

with $\overline{c}$ and δ_e represent the mean chord line and the elevator deflection, respectively.

III. Vertical Trajectory Tracking Control Objectives

Here our objectives are twofold:

- make the aircraft to follow accurately a space-referenced vertical profile $z_d(x)$ in accordance with economic and environmental constraints.

- make the aircraft to respect a desired time table $t_d(x)$ for its progress towards the runway in accordance with air traffic management considerations.

To meet directly this second objective in presence of wind could lead to hazardous situations with respect to airspeed limits as shown in Fig. 2 below, so this objective is shifted to the track of a desired airspeed. Here, it is supposed that online estimates of wind parameters are available (Sandeep S, Mulgund and Robert F, Stengel.1996).

From the desired time table $t_d(x)$, we get a desired ground speed $V_{G_d}(x)$:

$$V_{G_d}(x) = \frac{1}{\frac{dt_d}{dx}(x)} \tag{16}$$

then, tacking into account an estimate of the longitdinal component of wind speed, a space-referenced desired airspeed $V_{air_d}(x)$ can be defined:

- For low speeds, a minimum margin with respect to the stall speed at the current desired level:

$$V_{air_d}(x) = Max\left\{V_S(z_d(x)) + \Delta V_{min}, V_{Gd}(x) - \hat{w}_x(x)\right\} \tag{17}$$

where $V_S, \Delta V_{min}$ and $\hat{w}_x$ are the stall speed, the minimum margin speed and the estimate of the horizontal wind speed, respectively.

- For high speeds, an airspeed less than the maximum operating speed at the current desired level:

$$V_{air_d}(x) = Min\left\{V_{MO}(z_d(x)), V_{Gd}(x) - \hat{w}_x(x)\right\} \tag{18}$$

where V_{MO} denotes the maximum operating speed.

- In all other cases:

$$V_{air_d}(x) = V_{Gd}(x) - \hat{w}_x(x) \tag{19}$$

In the following section a nonlinear inverse control technique will be applied to the spatial dynamics of the aircraft which will be such as its tracking errors follow decoupled linear spatial dynamics such as:

$$\sum_{k=0}^{K} a_k\left(y^{[k]} - y_d^{[k]}\right) = 0 \tag{20}$$

where y is either $z(x)$ or $V_{air}(x)$ and y_d is the corresponding desired profile. $[k]$ denotes the k^{th} space derivative of the considered output $y(x)$ and $(K-1)$ is equal to the relative degree (Slotine, I.J. and Weiping, L.1991) of the output y.

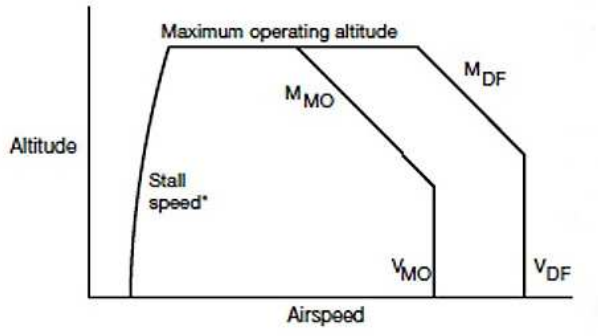

Figure 2. Example of civil aircraft aerodynamic operational flight envelope

IV. Space-Based NLI Tracking Control

The trajectory output variables equations can be written under an affine form with respect to the inputs q and T_C:

$$V_{air}^{[2]} = \frac{1}{V_G^2}\left[A_V(z,\alpha,V_{air},T,W) + B_{V_q}(z,\alpha,V_{air},T,W)q + B_{V_T}(z,\alpha,V_{air},T,W)T_C\right] \tag{21a}$$

$$z^{[3]} = \frac{1}{V_G^2}\left[A_z(z,\alpha,V_{air},T,W) + B_{z_q}(z,\alpha,V_{air},T,W)q + B_{z_T}(z,\alpha,V_{air},T,W)T_C\right] \tag{21b}$$

where W represent the parameters w_x, w_z, $\dot{w}_x$, $\dot{w}_z$ and $\ddot{w}_x$, $\ddot{w}_z$ which can be expressed successively (see Appendix).

Since the B_i terms shown below are in general not null, the spatial relative degree of V_{air} and z are equal respectively to 1 and 2, then in this case there are no internal dynamics to worry about.

The components A_V, B_{V_q}, B_{V_T} and A_z, B_{z_q}, B_{z_T} are given by:

$$\begin{aligned} A_V = \frac{1}{m}\Bigg[&-\frac{T}{\tau}\cos\alpha + T\dot{\gamma}_{air}\sin\alpha - \rho(z)V_{air}\dot{V}_{air}SC_X + \frac{1}{2}\rho(z)V_{air}^3S(C_1\dot{\gamma}_{air} + 2C_2\dot{\gamma}_{air}\alpha) \\ &+ W_{xx}(\ddot{x}\cos\gamma_{air} - \dot{x}\dot{\gamma}_{air}\sin\gamma_{air}) + W_{xz}(\ddot{z}\cos\gamma_{air} - \dot{z}\dot{\gamma}_{air}\sin\gamma_{air}) - W_{zx}(\ddot{x}\sin\gamma_{air} + \dot{x}\dot{\gamma}_{air}\cos\gamma_{air}) \\ &- W_{zz}(\ddot{z}\sin\gamma_{air} + \dot{z}\dot{\gamma}_{air}\cos\gamma_{air}) + \dot{W}_{xt}\cos\gamma_{air} - W_{xt}\dot{\gamma}_{air}\sin\gamma_{air} - \dot{W}_{zt}\sin\gamma_{air} - W_{zt}\dot{\gamma}_{air}\cos\gamma_{air} \\ &- \frac{\dot{V}_{air}}{V_G}(-\dot{V}_{air}\cos\gamma_{air} + V_{air}\dot{\gamma}_{air}\sin\gamma_{air} + W_{xx}\dot{x} + W_{xz}\dot{z} + W_{xt}) - mg\dot{\gamma}_{air}\cos\gamma_{air}\Bigg] \end{aligned} \tag{22a}$$

$$B_{V_q} = \frac{1}{m}\left[-T\sin\alpha - \frac{1}{2}\rho(z)V_{air}^2SC_1 - \rho(z)V_{air}^2SC_2\alpha\right] \tag{22b}$$

$$B_{V_T} = \frac{1}{m\tau}\cos\alpha \tag{22c}$$

and

$$\begin{aligned} A_z = \frac{1}{V_G^2}\Bigg[&A_V(w_x\sin\gamma_{air} + w_z\cos\gamma_{air}) + F(z,\alpha,V_{air},T,W)\Big\{-V_{air}^2 + V_{air}(w_x\cos\gamma_{air} - w_z\sin\gamma_{air})\Big\} \\ &+ \Upsilon(z,\alpha,V_{air},T,W)V_G^2\Bigg] \end{aligned} \tag{23}$$

with $\Upsilon(z,\alpha,V_{air},T,W)$ and $F(z,\alpha,V_{air},T,W)$ are such as:

$$\begin{aligned}\Upsilon = \frac{1}{V_G^2}\Bigg[&-2V_{air}\dot{V}_{air}\dot{\gamma}_{air} + 2\dot{V}_{air}\dot{\gamma}_{air}(w_x\cos\gamma_{air} - w_z\sin\gamma_{air}) - V_{air}\dot{\gamma}_{air}^2(w_x\sin\gamma_{air} + w_z\cos\gamma_{air})\\ &- V_{air}(\ddot{w}_z\cos\gamma_{air} + \ddot{w}_x\sin\gamma_{air}) + w_x(W_{zx}\ddot{x} + W_{zz}\ddot{z} + \dot{W}_{zt}) - w_z(W_{xx}\ddot{x} + W_{xz}\ddot{z} + \dot{W}_{xt})\\ &- \frac{2}{V_G}(-\dot{V}_{air}\cos\gamma_{air} + V_{air}\dot{\gamma}_{air}\sin\gamma_{air} + \dot{w}_x)\Bigg\{-V_{air}^2\dot{\gamma}_{air} - V_{air}(\dot{w}_z\cos\gamma_{air} + \dot{w}_x\sin\gamma_{air})\\ &+ V_{air}\dot{\gamma}_{air}(w_x\cos\gamma_{air} + w_z\sin\gamma_{air}) + \dot{V}_{air}(w_x\sin\gamma_{air} - w_z\cos\gamma_{air}) + w_x(W_{zx}\dot{x} + W_{zz}\dot{z} + W_{zt})\\ &+ w_z(W_{xx}\dot{x} + W_{xz}\dot{z} + W_{xt})\Bigg\}\Bigg]\end{aligned} \tag{24}$$

$$\begin{aligned}F = \frac{1}{mV_{air}}\Bigg[&-\frac{T}{\tau}\sin\alpha - T\dot{\gamma}_{air}\cos\alpha + \rho(z)V_{air}\dot{V}_{air}SC_Z - \frac{1}{2}\rho(z)V_{air}^2SC_{Z_\alpha}\dot{\gamma}_{air} + mg\dot{\gamma}_{air}\sin\gamma_{air}\\ &- m(\ddot{w}_x\sin\gamma_{air} + \dot{w}_x\dot{\gamma}_{air}\cos\gamma_{air} + \ddot{w}_z\cos\gamma_{air} - \dot{w}_x\dot{\gamma}_{air}\sin\gamma_{air})\\ &- \frac{m\dot{\gamma}_{air}}{V_G}\Bigg\{-V_{air}^2\dot{\gamma}_{air}\sin\gamma_{air} + \dot{V}_{air}w_x - V_{air}(W_{xx}\dot{x} + W_{xz}\dot{z} + W_{xt})\Bigg\}\Bigg]\end{aligned} \tag{25}$$

and

$$\begin{aligned}B_{z_q} = \frac{1}{V_G^2}\Bigg[&\frac{1}{m}(w_x\sin\gamma_{air} + w_z\cos\gamma_{air})\left(-T\sin\alpha - \frac{1}{2}\rho(z)V_{air}^2SC_1 - \rho(z)V_{air}^2SC_2\alpha\right)\\ &+ \frac{1}{mV_{air}}\Bigg\{-V_{air}^2 + V_{air}(w_x\cos\gamma_{air} - w_z\sin\gamma_{air})\Bigg\}\left(T\cos\alpha + \frac{1}{2}\rho(z)V_{air}^2SC_{Z_\alpha}\right)\Bigg]\end{aligned} \tag{26a}$$

$$B_{z_T} = \frac{1}{V_G^2}\left[\frac{\cos\alpha}{m\tau}(w_x\sin\gamma_{air} + w_z\cos\gamma_{air}) + \frac{\sin\alpha}{mV_{air}\tau}\Bigg\{-V_{air}^2 + V_{air}(w_x\cos\gamma_{air} - w_z\sin\gamma_{air})\Bigg\}\right] \tag{26b}$$

In the above equations $\dot{u}$ and $\ddot{u}$ with $u \in \{x, z, \gamma_{air}, V_{air}, w_x, w_z\}$ denote quantities:

$$\dot{u} = u^{[1]}V_G \tag{27a}$$

$$\ddot{u} = u^{[2]}{V_G}^2 + u^{[1]}V_G^{[1]}V_G \tag{27b}$$

The desired vertical trajectory $z_d(x)$ is supposed to be a smooth function of x (distance to touchdown) while considering expressions (17), (18) and (19) V_{air_d} is supposed to be an almost everywhere smooth function of x.

Now, let $\xi_z(x)$ and $\xi_{V_{air}}(x)$ be the tracking errors related to the desired altitude $z_d(x)$ and desired airspeed profile $V_{air_d}(x)$, respectively:

$$\xi_z(x) = z(x) - z_d(x) \tag{28a}$$

$$\xi_{V_{air}}(x) = V_{air}(x) - V_{air_d}(x) \tag{28b}$$

Then, considering equations (21a) and (21b), the following linear decoupled space dynamics can be chosen as control objectives:

$$V_{air}^{[2]}(x) = V_{air_d}^{[2]}(x) + k_{1v}\xi_{V_{air}}^{[1]}(x) + k_{2v}\xi_{V_{air}}(x) \tag{29a}$$

$$z^{[3]}(x) = z_d^{[3]}(x) + k_{1z}\xi_z^{[2]}(x) + k_{2z}\xi_z^{[1]}(x) + k_{3z}\xi_z(x) \tag{29b}$$

where $k_{1v}, k_{2v}, k_{1z}, k_{2z}$ and k_{3z} are real parameters such as the roots of $p^2 + k_{1v}p + k_{2v}$ and $p^3 + k_{1z}p^2 + k_{2z}p + k_{3z}$ produce adequate tracking error dynamics (convergence without oscillation in accordance with a given space segment) with p denotes the Laplace variable.

Since in normal flight conditions the control matrix given by:

$$\begin{pmatrix} B_{z_q} & B_{z_T} \\ B_{V_q} & B_{V_T} \end{pmatrix} \tag{30}$$

is invertible, it is possible to proceed by dynamic inversion to get a trajectory tracking control laws (Isidori, A.1989), (Slotine, I.J. and Weiping, L.1991).

The nonlinear dynamic inversion technique produces the following spatial control laws for q and T_C as:

$$\begin{pmatrix} q(x) \\ T_C(x) \end{pmatrix} = \begin{pmatrix} B_{z_q} & B_{z_T} \\ B_{V_q} & B_{V_T} \end{pmatrix}^{-1} \begin{pmatrix} V_G^2 \left[z_d^{[3]}(x) + k_{1z}\xi_z^{[2]}(x) + k_{2z}\xi_z^{[1]}(x) + k_{3z}\xi_z(x) \right] - A_z \\ V_G^2 \left[V_{air_d}^{[2]}(x) + k_{1v}\xi_{V_{air}}^{[1]}(x) + k_{2v}\xi_{V_{air}}(x) \right] - A_V \end{pmatrix} \tag{31}$$

Observe here that while the successive spatial derivatives of $z_d(x)$ and $V_{aird}(x)$ can be directly computed, the successive spatial derivatives of $z(x)$ and $V_{air}(x)$ in (29a) and (29b) can be computed from relations (12a), (12d) and (13) where the wind parameters are replaced by their estimates.

V. Space-Based Versus Time-Based NLI Tracking Control

In the litterature, the nonlinear inverse control technique has been applied to trajectory tracking using time as the independant variable (Isidori, A.1989). In this section, it is shown briefly that there is in general no equivalent time base linear decoupled dynamics to equations (29a) and (29b) with respect to altitude and airspeed.

According to derivative rules for composed functions, it is possible to write:

$$\xi_z^{[1]} = \frac{\dot{\xi}_z}{V_G} \tag{32a}$$

$$\xi_z^{[2]} = \frac{1}{{V_G}^2}\left(\ddot{\xi}_z - \frac{\dot{\xi}_z \dot{V}_G}{V_G} \right) \tag{32b}$$

$$\xi_z^{[3]} = \frac{1}{{V_G}^3}\left[\dddot{\xi}_z - 3\ddot{\xi}_z \frac{\dot{V}_G}{V_G} + \dot{\xi}_z \left(3\frac{\dot{V}_G^2}{{V_G}^2} - \frac{\ddot{V}_G}{V_G} \right) \right] \tag{32c}$$

and

$$\xi_{V_{air}}^{[1]} = \frac{\dot{\xi}_{V_{air}}}{V_G} \tag{33a}$$

$$\xi_{V_{air}}^{[2]} = \frac{1}{{V_G}^2}\left(\ddot{\xi}_{V_{air}} - \frac{\dot{\xi}_{V_{air}} \dot{V}_G}{V_G} \right) \tag{33b}$$

where:

$$V_G(x(t)) = -\left(V_{aird}(x(t)) + \xi_{V_{air}}(x(t)) \right) \sqrt{1 - \left(\frac{\dot{z}_d(x(t)) + \dot{\xi}_z(x(t)) - w_z(x(t))}{V_{aird}(x(t)) + \xi_{V_{air}}(x(t))} \right)^2} + w_x(x(t)) \tag{34}$$

Then, it appears that when replacing in equations (29a) and (29b) the space derivatives of the output by the expressions given by (32a) to (33b), we will get nonlinear and non decoupled time dynamics for the altitude and the airspeed errors.

However, in the case of a constant ground speed, the space and temporal derivatives are related by:

$$\xi_z^{[k]} = \frac{\xi_z^{(k)}}{{V_G}^k} \tag{35a}$$

$$\xi_{V_{air}}^{[k]} = \frac{\xi_{V_{air}}^{(k)}}{{V_G}^k} \tag{35b}$$

and we get the equivalent linear decoupled time dynamics:

$$\dddot{\xi}_z + k_{1z} V_G \ddot{\xi}_z + k_{2z} {V_G}^2 \dot{\xi}_z + k_{3z} {V_G}^3 \xi_z = 0 \tag{36a}$$

$$\ddot{\xi}_{V_{air}} + k_{1v} V_G \dot{\xi}_{V_{air}} + k_{2v} {V_G}^2 \xi_{V_{air}} = 0 \tag{36b}$$

A case in which the ground speed remains constant for some time (and space) is when the airspeed is maintained constant in no wind situation. Figures. 3 and 4 represent respectively airspeed profiles for conventional and continuous descent approach (CDA).

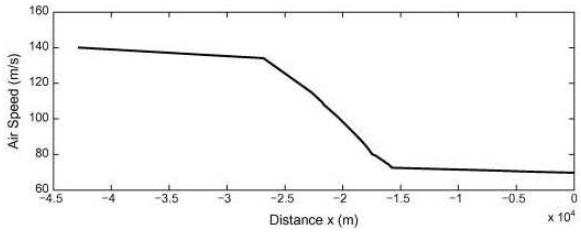

Figure 3. Example of conventional approach airspeed profile

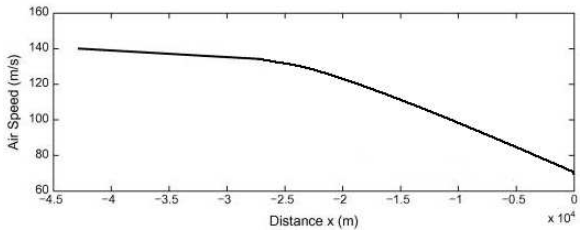

Figure 4. Example of CDA airspeed profile

In the case in which it is $\dot{V}_G$ which remains constant over a time (space) span, equations (36a) and (36b) becomes:

$$\dddot{\xi}_z + \left(k_{1z}V_G - 3\frac{\dot{V}_G}{V_G}\right)\ddot{\xi}_z + \left(k_{2z}{V_G}^2 - k_{1z}\dot{V}_G + 3\frac{\dot{V}_G^2}{{V_G}^2}\right)\dot{\xi}_z + k_{3z}{V_G}^3\xi_z = 0 \tag{37a}$$

$$\ddot{\xi}_{V_{air}} + \left(k_{1v}V_G - \frac{\dot{V}_G}{V_G}\right)\dot{\xi}_{V_{air}} + k_{2v}{V_G}^2\xi_{V_{air}} = 0 \tag{37b}$$

Here V_G is such as:

$$V_G(t) = V_G(t_0) + \dot{V}_G.(t - t_0) \tag{38}$$

with $\dot{V}_G = Constant$, then the above decoupled dynamics are with time variant parameters and the predictivity (time of response) of these dynamics is lost. It can be however shown that if $\dot{V}_G$ remains very small with respect to V_G, these dynamics are stable.

VI. Simulation Study

The proposed control approach is illustrated using the Research Civil Aircraft Model (RCAM) which has the characteristics of a wide body transportation aircraft (Magni J-F. et al.,1997) with a maximum allowable landing mass of about 125 tons with a nominal landing speed of 70m/s.

There, the control signals are submitted to rate limits and saturations (Magni J-F. et al.,1997) as follows:

$$-15\frac{\pi}{180}rad/s \leqslant \dot{\delta}_e \leqslant 15\frac{\pi}{180}rad/s \tag{39a}$$

$$-25\frac{\pi}{180}rad \leqslant \delta_e \leqslant 10\frac{\pi}{180}rad \tag{39b}$$

$$-1.6\frac{\pi}{180}rad/s \leqslant \dot{T}_C \leqslant 1.6\frac{\pi}{180}rad/s \tag{39c}$$

$$0.5\frac{\pi}{180}rad \leqslant T_C \leqslant 10\frac{\pi}{180}rad \tag{39d}$$

while the minimum allowable speed is $1.23 \times V_{stall}$ with $V_{stall} = 51.8$m/s and the angle of attack is limited to the interval $[-11.5°, 18°]$ where $\alpha_{stall} = 18°$.

Examples of reference altitude and airspeed trajectories are displayed in Fig. 5. These trajectories are given by polynomial functions of space distance to the runway x and are such as desired altitude and airspeed vary continuously

from initial to final values according with the continuous descent approach (CDA) philosophy. The desired trajectories start at the altitude of 3000m with an airspeed of 140m/s. At the altitude of 1000m with an airspeed of 90m/s and with a path angle of -3°, the desired trajectory joins the glide path towards the runway.

With respect to guidance objectives, spatial error dynamics have been chosen so that the tracking error goes to zero without overshooting or oscillations. To get an average additional path angle of -6° during convergence, the convergence distance has been taken equal to 2500m which corresponds to about 18s flown at initial desired speed. Once coefficients k_{iv}, $i = 1, 2$ and k_{iz}, $i = 1$ to 3 in (29a) and (29b) have been chosen with the above objective, time error dynamics have been taken in (36a) and (36b) with a value of V_G equal to 80m/s.

A. Simulation results in no wind condition

In a no wind condition, Fig. 6a and Fig. 6b display altitude and airspeed tracking performances when nonlinear inversion is performed according to space, while Fig. 7a and Fig. 7b display the corresponding tracking performances when nonlinear inversion is done with respect to time. Since except at initial transients the performances look similar, Fig. 8 and Fig. 9 provide closer views of altitude and airspeed tracking performances during initial transients. It appears clearly that in both cases the new NLI trajectory tracking technique provides better results: the spatial span for convergence towards the desired trajectories is shortened by about 2000m while convergence is performed with reduced oscillations.

Figures. 10, 11 and 12 display the evolution of respectively the angle of attack α, the elevator deflection δ_e and the throttle setting T_C during the whole maneouver. Since α remains in a safe domain and the considered longitudinal inputs remain by far unsaturated this demonstrates the feasibility of the manoeuver.

B. Simulation results in the presence of wind

A tailwind with a mean value of 12m/s has been considered. Its horizontal and vertical components are given by:

$$w_x = W_x(z) + \delta_x(V_{air}, z, t) \tag{40a}$$

$$w_z = \delta_z(V_{air}, z, t) \tag{40b}$$

where $\delta_x(V_{air}, z, t)$ and $\delta_z(V_{air}, z, t)$ are stochastic components. The deterministic part $W_x(z)$ as well as the stochastic parts δ_x and δ_z are generated according to the wind model described in the appendix. Figure. 13 provide an example of realization of such wind.

Since in this study the problem of the online estimation of the wind components has not been tackled, it has been supposed merely that the wind estimator will be similar to a first order filter with a time constant equal to 0.35s in one case and with a space constant equal to 28m in the other case. Then the filtered values of these wind components have been fed to the respective NLI control laws.

Figures. 14, 15, 16, 17 and 18 represent the evolution of the aircraft parameters under either space NLI or time NLI. These results can be compared with those of Fig. 8, 9, 10, 11 and 12 in the no wind condition. It appears that the performances of the system are slightly downgraded in the presence of wind. The superiority of the space NLI control over the time NLI control is much more pronounced now since in the first case the angle of attack (Fig. 16) remains in a safe domain, which is not the case with the second technique and the elevator deflection remains largely unsaturated in the first case and comes near saturation level in the second case (Fig. 17).

VII. Conclusion

In this communication a new vertical guidance scheme for transportation aircraft has been proposed. The main objective here has been to improve the tracking accuracy performance of the guidance along a desired trajectory referenced in a spatial frame. This has led to develop a new representation of vertical flight dynamics where the independant variable is ground distance. The classical nonlinear inverse control technique has been applied in this content so that tracking errors follow independant and asymptotically stable spatial dynamics around the desired trajectories. It has been shown that a similar tracking objective expressed in the time frame cannot be equivalent when the desired airspeed changes as it is generally the case along climb and approach for landing.

Tracking performances obtained from spatial and time NLI guidance have been compared through a simulation study considering a descent manoeuver of a transportation aircraft in wind and no wind conditions. It appears already that the proposed approach induces improved tracking performances as well as a new spatial predictability.

To gain applicability this new guidance approach should overcome important difficulties related mainly with navigation and online wind estimation inaccuracies. Then an improved integration of on board flight path optimization functions including neighbouring traffic and the guidance function will become possible.

Appendix

In this study, vertical wind is given here according to (Etkin, B.1972) and (Frost, W. and Bowles, R.1984) as:

$$w_z = W_z(x,z,t) = \delta_z(V_{air},z,t) \tag{41a}$$

$$w_x = W_x(x,z,t) = W_x(z) + \delta_x(V_{air},z,t) \tag{41b}$$

where $W_x(z)$ and $\delta_{x,z}(V_{air},z,t)$ represent the deterministic and stochastic components of the considered wind, respectively.

The deterministic wind speed component is expressed as:

$$W_x(z) = W_0(z)\ln\left(\frac{z}{z_0}\right) \tag{42a}$$

$$W_0(z) = W_0^*\cos(\omega z + \varphi_0) \tag{42b}$$

where ω and W_0^* denote the circular space frequency and magnitude of the considered wind component.

The stochastic wind components adopt Dryden spectrum (Campbell, C. W.1984) generated from two unitary white gaussian noise processes through linear filters such as:

$$H_{\delta_x}(s) = \sigma_x\sqrt{\frac{2L_{xx}}{V_{air}}}\frac{1}{1+\frac{L_{xx}}{V_{air}}s} \tag{43}$$

and

$$H_{\delta_z}(s) = \sigma_z\sqrt{\frac{L_{zz}}{V_{air}}}\frac{1+\sqrt{3}\frac{L_{zz}}{V_{air}}s}{\left(1+\frac{L_{zz}}{V_{air}}s\right)^2} \tag{44}$$

Here L_{xx} and L_{zz} are shape parameters (turbulence lenghts) such as:

- For $z \leq 305$m:

$$L_{xx} = \frac{z}{(0.177+0.0027z)^{1.2}} \tag{45a}$$

$$L_{zz} = z \tag{45b}$$

- For $z > 305$m:

$$L_{xx} = L_{zz} = 305m \tag{46}$$

where σ_x and σ_z represent standard deviations of independant processes such as:

$$\sigma_z = 0.1W_{20} \tag{47}$$

and W_{20} is the horizontal wind speed at 20ft above ground level.

- For $z \leq 305$m:

$$\sigma_x = \frac{\sigma_z}{(0.177+0.0027z)^{0.4}} \tag{48}$$

- For $z > 305$m:

$$\sigma_x = \sigma_z \tag{49}$$

Time and spatial derivatives of the wind components are then given by:

$$\dot{w}_x = W_{xx}\dot{x} + W_{xz}\dot{z} + W_{xt} \tag{50}$$

with:

$$W_{xx} = \frac{\partial W_x}{\partial x} \qquad W_{xz} = \frac{\partial W_x}{\partial z} \qquad W_{xt} = \frac{\partial W_x}{\partial t} \tag{51}$$

and

$$\dot{w}_z = W_{zx}\dot{x} + W_{zz}\dot{z} + W_{zt} \tag{52}$$

with:

$$W_{zx} = \frac{\partial W_z}{\partial x} \qquad W_{zz} = \frac{\partial W_z}{\partial z} \qquad W_{zt} = \frac{\partial W_z}{\partial t} \tag{53}$$

References

[1]Miele A, et al, *Optimization and Gamma/Theta Guidance of Flight Trajectories in a Windshear*, Presented at the 15th ICAS Congress, London, 1986.

[2]Miele A, et al, *Guidance Strategies for Near-Optimum Takeoff Performance in Wind Shear*, Journal of Optimization Theory and Applications, Vol. 50, No. 1, 1986.

[3]Psiaki M.L. and R.F. Stengel, *Analysis of Aircraft Control Strategies for Microburst Encounter*, Journal of Guidance, Control, and Dynamics, Vol. 8, No. 5, p. 553-559, 1985.

[4]Miele A, et al, *Optimal Trajectories and Guidance Trajectories for Aircraft Flight Through Windshears*, Proceedings of the 29th Conference on Decision and Control, Honolulu, Hawaii, pp. 737-746, 1990.

[5]Psiaki M.L. and R.F. Stengel, *Optimal Aircraft Performance During Microburst Encounter*, Journal of Guidance, Control, and Dynamics, Vol. 14, No. 2, p. 440-446, 1991.

[6]Stengel, R.F, *Toward Intelligent Flight Control*, IEEE Trans. on Systems, Man, and Cybernetics, Vol. 23, No. 6, p. 1699-1717, 1993.

[7]Singh S.N. and W.J. Rugh, *Decoupling in a Class of Nonlinear Systems by State Feedback*, ASME Journal of Dynanmic Systems, Measurement, and Control, Series G, Vol. 94, p. 323-329, 1972.

[8]Sandeep S. Mulgund and Robert F. Stengel, *Optimal Nonlinear Estimation for Aircraft Flight Control in Wind Shear*, Automatica, Vol. 32, No. 1, January 1996.

[9]Psiaki M.L, *Control of Flight Through Microburst Wind Shear Using Deterministic Trajectory Optimization*, Ph.D. Thesis, Department of Mechanical and Aerospace Engineering, Princeton University, Report No. 1787-T, 1987.

[10]Psiaki M.L. and K. Park, *Thrust Laws for Microburst Wind Shear Penetration*, Journal of Guidance, Control, and Dynamics, Vol. 15, No. 4, 1992.

[11]I.J.-J. Slotine and L. Weiping, *Applied Nonlinear Control*, Prentice Hall, Upper Saddle River, NJ, 1991.

[12]Isidori A, *Nonlinear Control Systems*, Springer-Verlag, Berlin.

[13]Magni J-F. et al, *Robust Flight Control, A Design Challenge*, Springer-Verlag, London.

[14]Etkin B, *Dynamics of Atmospheric Flight*, John Wiley and Sons, Inc, New York, 1985.

[15]Frost W. and Bowles. R, *Wind Shear Terms in the Equations of Aircraft Motion*, Journal of Aircraft, Vol. 21, No.11, p. 866-872, 1984.

[16]Campbell C. W, *A Spatial Model of Wind Shear and Turbulence for Flight Simulation*, Tech. Rep. TP-2313, NASA George C. Marshall Space Flight Center, Alabama 35812, May 1984.

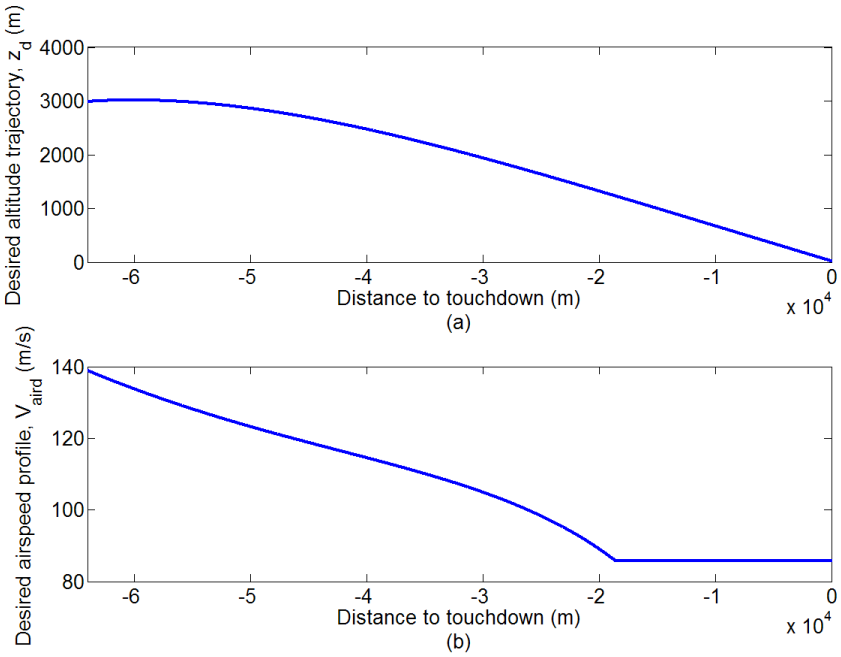

Figure 5. Desired altitude trajectory (a) and airspeed profile (b), respectively

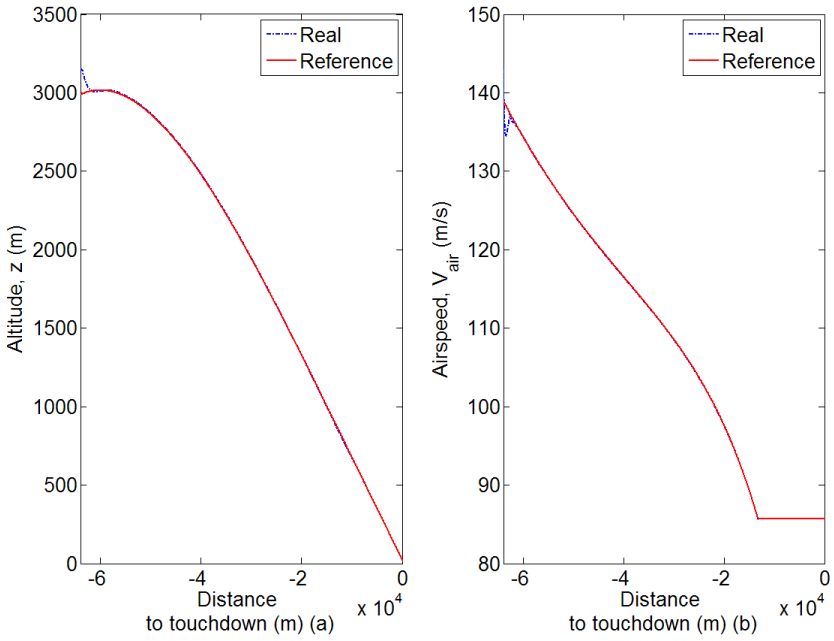

Figure 6. Altitude (a) and airspeed (b) tracking performances by space NLI.

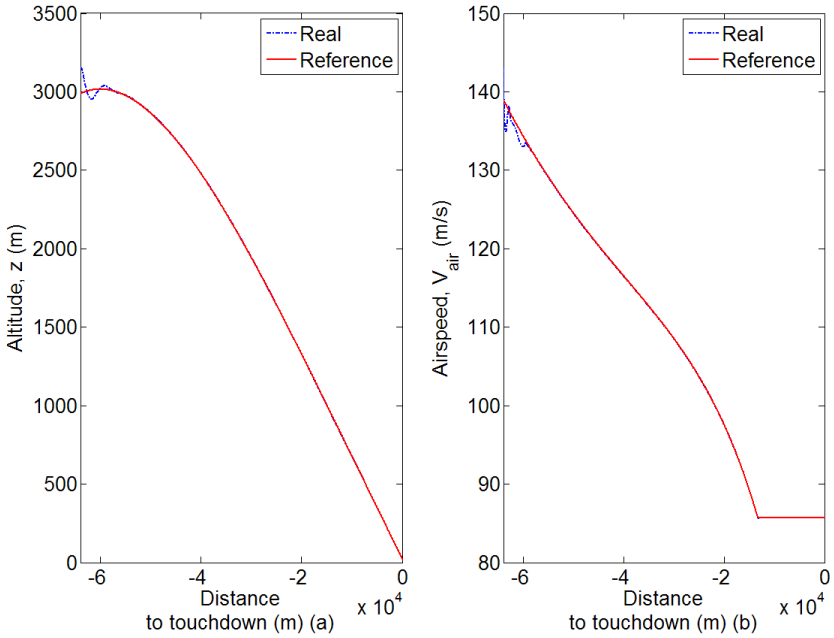

Figure 7. Altitude (a) and airspeed (b) tracking performances by time NLI.

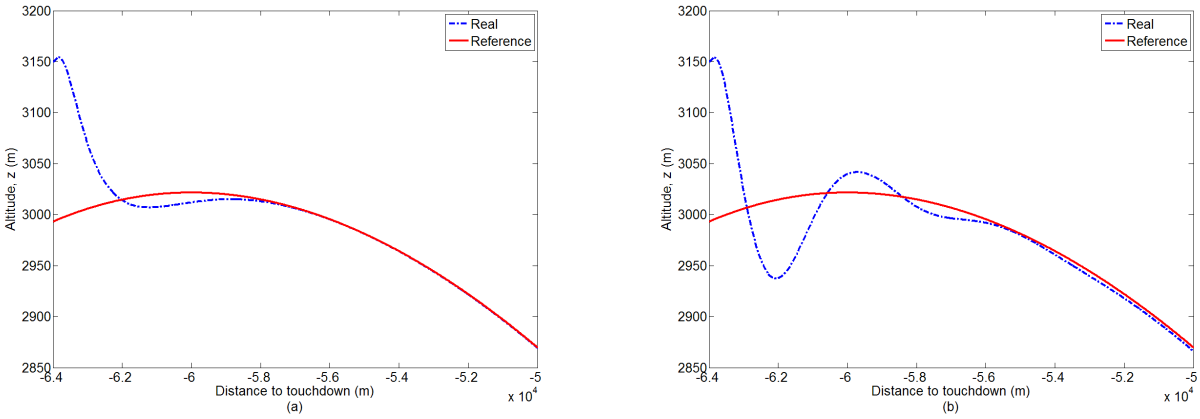

Figure 8. Initial altitude tracking by space NLI (a) and time NLI (b), (no wind).

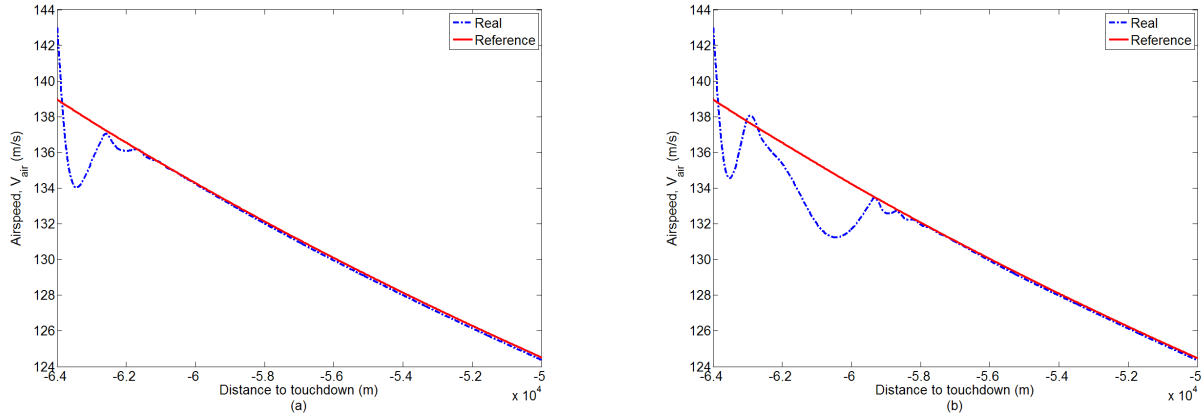

Figure 9. Initial airspeed tracking by space NLI (a) and time NLI (b), (no wind).

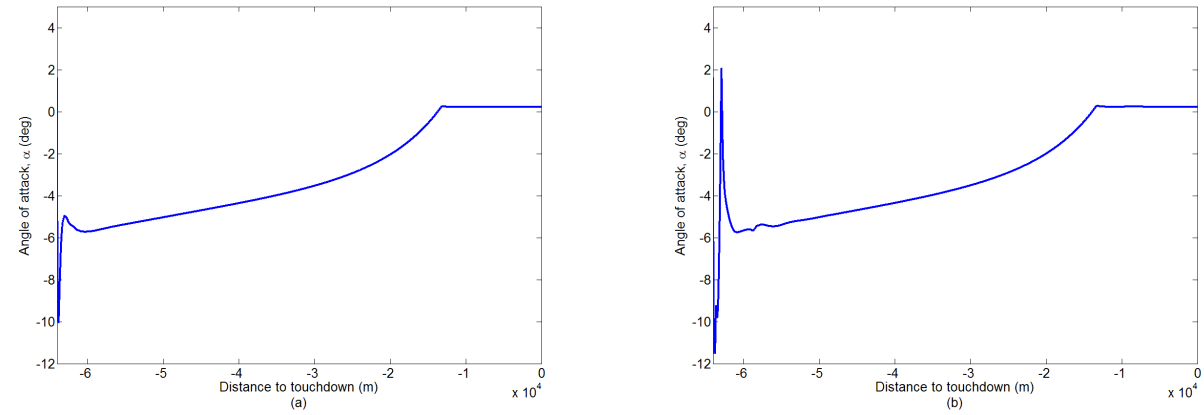

Figure 10. Angle of attack evolution with space NLI (a) and with time NLI (b), (no wind).

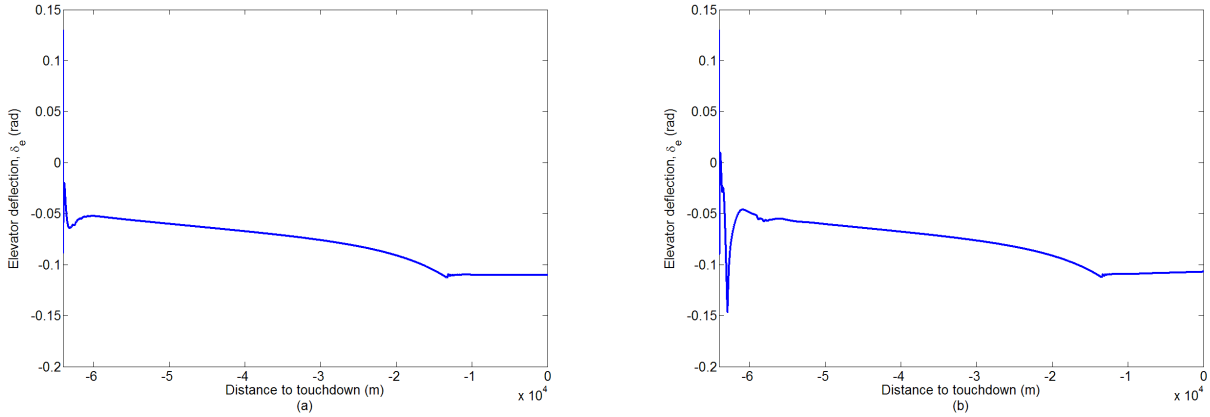

Figure 11. Elevator deflection evolution with space NLI (a) and with time NLI (b), (no wind).

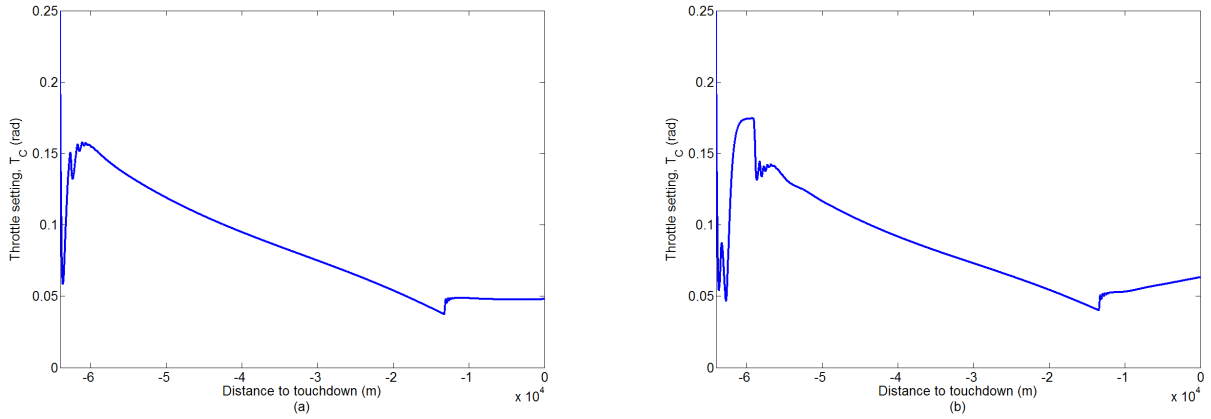

Figure 12. Throttle setting evolution with space NLI (a) and with time NLI (b), (no wind).

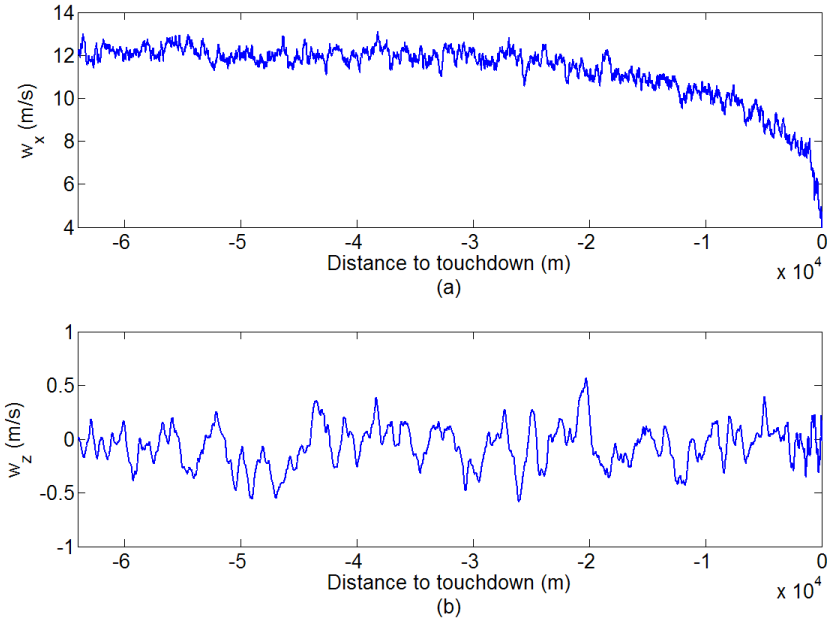

Figure 13. Example of wind components realization

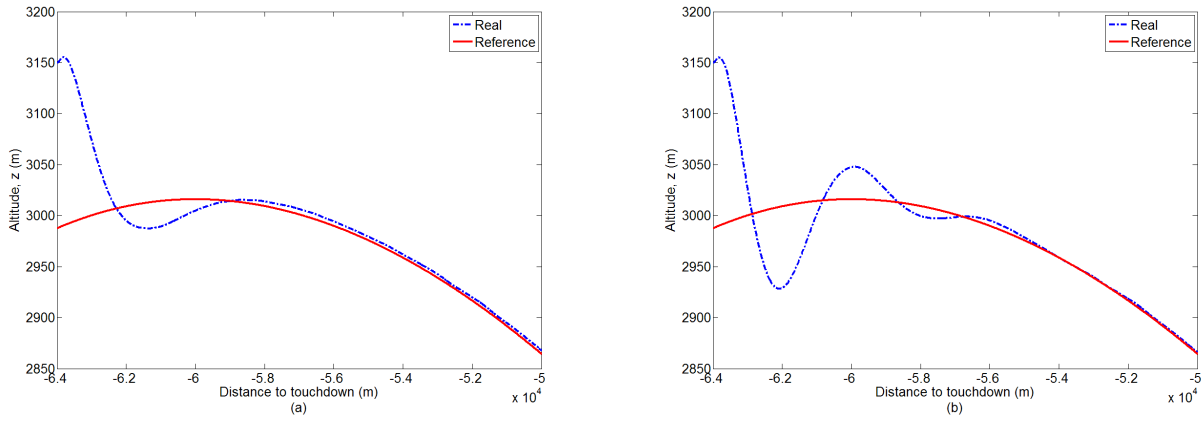

Figure 14. Initial altitude tracking by space NLI (a) and time NLI (b), (with wind).

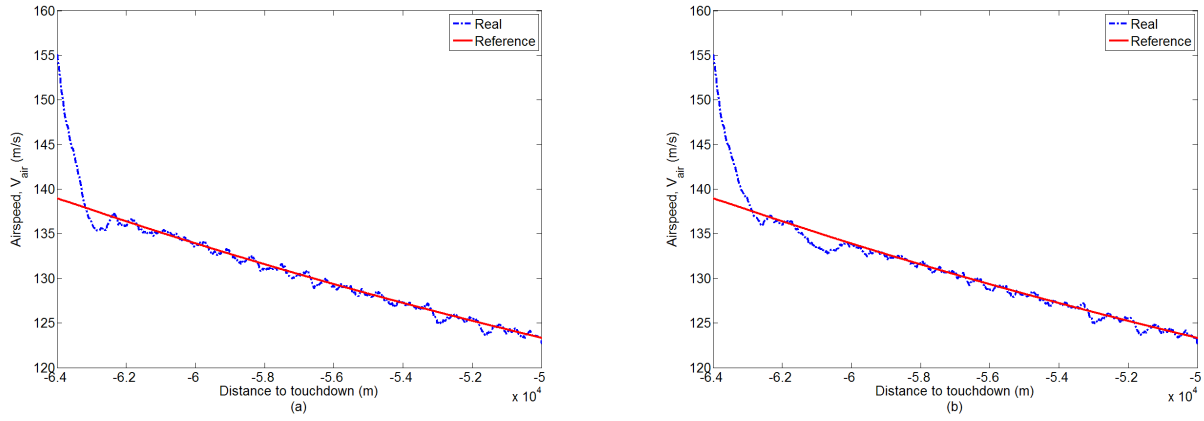

Figure 15. Initial airspeed tracking by space NLI (a) and time NLI (b), (with wind).

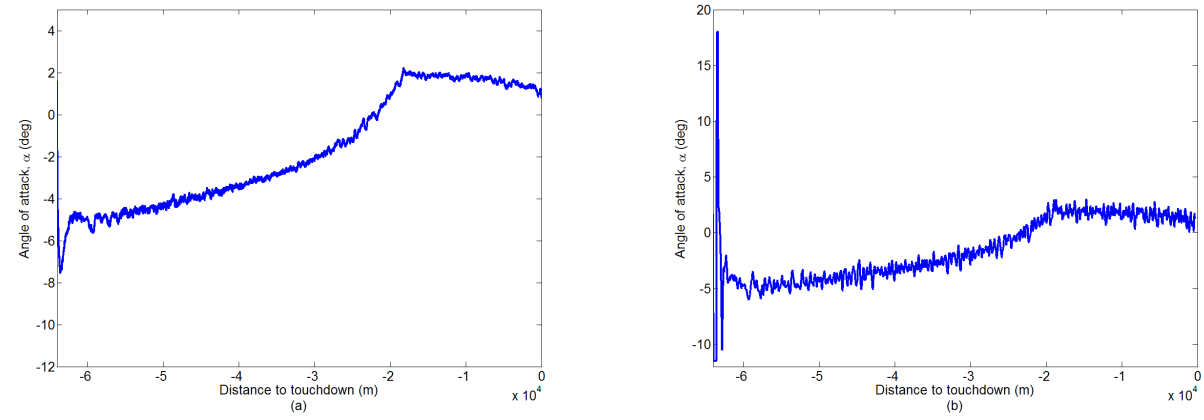

Figure 16. Angle of attack evolution with space NLI (a) and with time NLI (b), (with wind).

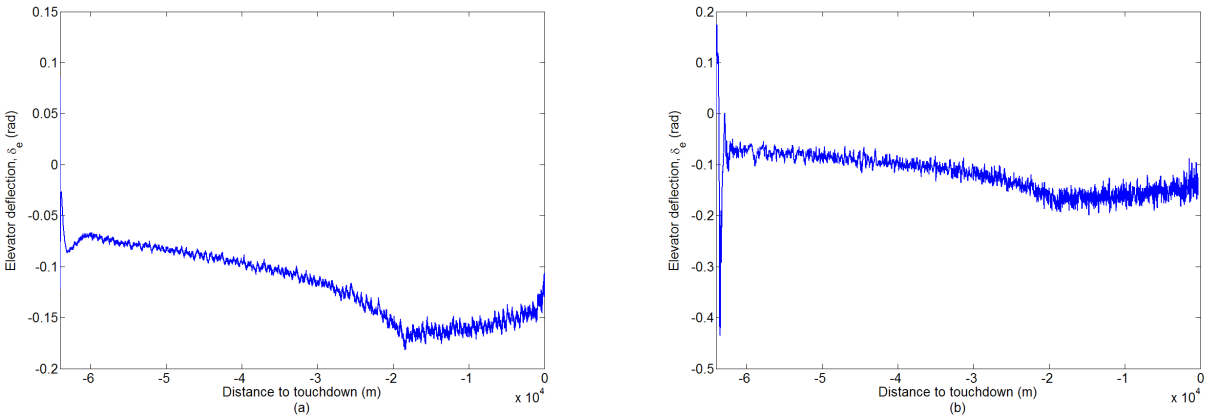

Figure 17. Elevator deflection evolution with space NLI (a) and with time NLI (b), (with wind).

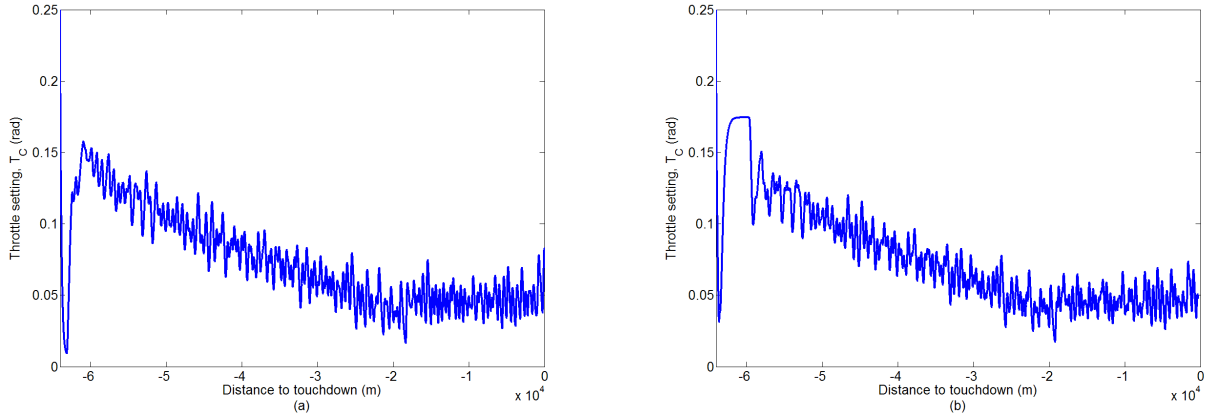

Figure 18. Throttle setting evolution with space NLI (a) and with time NLI (b), (with wind).